Published in final edited form as:
Sci Signal. ; 3(119): ra33. doi:10.1126/scisignal.2000800.

Evolution of CASK into a Mg^{2+}-sensitive kinase

Konark Mukherjee[1,4,*], **Manu Sharma**[1], **Reinhard Jahn**[2], **Markus C. Wahl**[3,*], and **Thomas C. Südhof**[1,*]

[1]Dept. of Mol. and Cellular Physiology Stanford University School of Medicine 1050 Arastradero Rd. Palo Alto, CA 94304, USA

[2]Max-Planck-Institut für Biophysikalische Chemie Neurobiologie Am Faßberg 11 D-37077 Göttingen, Germany

[3]Freie Universität Berlin Fachbereich Biologie, Chemie, Pharmazie Institut für Chemie und Biochemie AG Strukturbiochemie Takustr. 6, D-14195 Berlin, Germany

SUMMARY

All known protein kinases, except CASK, require Mg^{2+} to stimulate phosphotransfer from ATP to a protein substrate. The CaM-kinase domain of CASK exhibits activity in the absence of Mg^{2+}, moreover it is inhibited by divalent ions including Mg^{2+}. Here, we converted the Mg^{2+}-inhibited wild type CASK kinase ($CASK^{WT}$) into a Mg^{2+}-stimulated kinase ($CASK^{4M}$) by substituting four residues within the ATP-binding pocket. Crystal structures of $CASK^{4M}$ with and without bound nucleotide and Mn^{2+}, together with kinetic analyses demonstrate that Mg^{2+} accelerates catalysis of $CASK^{4M}$ by stabilizing the transition state, enhancing the leaving group properties of ADP and by productive positioning the γ-phosphate of ATP. Phylogenetic analysis revealed that the four residues conferring Mg^{2+}-mediated stimulation were lost from CASK during early animal evolution, converting a primordial, Mg^{2+}-coordinating CASK into a Mg^{2+}-inhibited kinase. This emergence of Mg^{2+}-sensitivity conferred divalent ion-driven regulation to CASK, in parallel with the evolution of animal nervous systems.

INTRODUCTION

Protein kinases comprise approximately 1.7 % of the protein-coding genes in the human genome (1) and are valuable targets for therapeutics (2). Structural and functional similarities among diverse eukaryotic protein kinases suggest that they evolved from a common ancestor. Thus, protein kinases exhibit an N-terminal lobe, comprised of five-stranded, antiparallel β-sheet and a regulatory helix, αC, and a largely α-helical C-terminal lobe (3). The enzymes employ a number of highly conserved functional motifs to exert substrate peptide binding, nucleotide binding and catalysis (3). These motifs include an Asp-Phe-Gly (DFG) sequence at the beginning of the activation segment and a conserved asparagine in the catalytic loop of the C-terminal lobe, which are involved in Mg^{2+}-binding and were believed to be indispensable for the catalysis of phosphotransfer by kinases (4,3,5). During evolution, some kinases acquired mutations in some of the conserved functional motifs. Non-canonical motifs may satisfy unique functional requirements in particular kinases, such as an unusual substrate specificity, or confer particular catalytic properties

[*]To whom correspondence should be addressed. TCS: Tel.: 650-721-1421; Fax: 650-498-4585; tcs1@stanford.edu KM: Tel.: 214-649-7157; Fax: 650-498-4585; konark@Brandeis.edu MCW: Tel.: +49-30-838-53456; Fax: +49-30-838-56981; mwahl@chemie.fu-berlin.de.
[4]Current address: Biology Department Brandeis University, MS008 415 South Street Waltham, MA 02454-9110

EXPERIMENTAL PROCEDURES See supplemental material for Methods.

(6,7). Some changes may also be detrimental to catalysis and about 10 % of the human protein kinases bearing such changes are presently classified as “pseudokinases” (8). However, despite their presumed catalytic inactivity, most pseudokinases, for example Her-3, Jak-2, CCK4 and IRAK2, are essential and are thought to regulate the function of other active kinases.

Many protein kinases bear additional domains or regions, which can regulate a kinase via autoinhibition, oligomerization or recruitment of substrates (9). Thus, while a fundamental level of regulation is implemented via the conserved functional motifs within the kinase domain, additional domains provide another layer of regulation from outside of the kinase core.

CASK is an essential protein that contains an N-terminal protein kinase domain, followed by elements characteristic of membrane-associated guanylate kinases (MAGUKs), including a PDZ-, an SH3- and an inactive guanylate kinase domain. CASK is highly enriched in brain where it binds to cell-adhesion molecules, including neurexins (10), syndecans (11,12,13) and SynCAM (14). In mice, genetic disruption of CASK causes a cleft palate, synaptic dysfunction and lethality (15). In humans, mutations in the *CASK* gene also produce a cleft palate syndrome with optic atrophy and mental retardation (16,17,18,19,20).

The N-terminal kinase domain of CASK most closely resembles members of the sub-family of Ca^{2+}/calmodulin (CaM)-dependent protein kinases. However, human CASK exhibits a Gly162-Phe163-Gly164 (GFG) instead of the Mg^{2+}-binding DFG motif and a cysteine (Cys146) instead of the conserved, Mg^{2+}-binding asparagine in the catalytic loop. Consistent with these substitutions, Mg^{2+}-binding in CASK is disrupted (21). Since Mg^{2+} was considered an indispensable cofactor for catalytic phosphotransfer, CASK was categorized as a pseudokinase (Boudeau *et al.*, 2006). Recently, however, we found that CASK binds ATP and catalyzes phosphotransfer to the synaptic adhesion molecule neurexin-1, even in the absence of Mg^{2+} (21). Indeed, CASK is fully active only in the absence of divalent cations such as Mg^{2+} and Ca^{2+} (21). The inhibition of CASK by divalent metal ions would provide an effective mechanism to allow CASK activity in inactive neurons (low divalent ion concentration) and to shut down the enzyme in active neurons (high divalent ion concentration) (21).

To gain insight into how the unique Mg^{2+}-sensitive catalytic activity of CASK evolved, we have carried out systematic mutagenesis, mechanistic and structural studies. We found that substitutions of four residues, generating $CASK^{4M}$, turn CASK into a Mg^{2+}-stimulated kinase. However unlike conventional kinases, $CASK^{4M}$ retained significant Mg^{2+}-independent phosphotransfer activity. Structural analysis revealed that in $CASK^{4M}$, Mg^{2+} accelerates catalysis by stabilizing the transition state, by enhancing the leaving group properties of ADP and by indirectly positioning the γ-phosphate of ATP, suggesting a similar role for Mg^{2+} in conventional protein kinases. Although strongly stimulated by Mg^{2+}, $CASK^{4M}$ exhibited the comparable activity towards neurexin-1 as $CASK^{WT}$ *in vivo*, suggesting that the divalent ion-sensitive kinase activity of CASK is an adaptive innovation that serves to convert CASK from a general kinase into a kinase specific for substrates that are recruited via its MAGUK domains. Strikingly, evolutionary comparison of CASK sequences demonstrates that CASK initially emerged as a Mg^{2+}-utilizing kinase, and later became Mg^{2+}-sensitive. The amino acid substitutions that rendered CASK sensitive to Mg^{2+} occurred during early animal evolution, in parallel with the appearance of the nervous system. Thus, CASK represents a case, in which apparently detrimental changes in conserved functional motifs do not lead to the loss of catalytic activity but instead may have implemented a novel regulatory mechanism.

RESULTS

Designing a Mg^{2+}-coordinating version of CASK

The CASK CaM-kinase domain is highly homologous to the corresponding domains of canonical CaM-kinases, such as CaMKI (≈ 37% identity) and CaMKII (≈ 44% identity) (1). CaMKI and CaMKII need Mg^{2+} and Ca^{2+} for optimal activity. Mg^{2+} activates phosphotransfer from ATP, while Ca^{2+} is required for activation of calmodulin, which counteracts autoinhibition of the enzymes. In contrast, the CASK CaM-kinase domain is inhibited by Mg^{2+} or Ca^{2+} and no metal ion was found in crystal structures of the CASK CaM-kinase domain in complex with adenine nucleotides (21).

Sequence alignments of vertebrate CASKs with human CaMKI and CaMKII reveal substitutions in CASK of residues that are highly conserved in canonical CaM-kinases; *i.e.* the Mg^{2+}-coordinating aspartate of the DFG motif is replaced by a glycine (Gly162), and the Mg^{2+}-binding asparagine of the catalytic-loop is replaced by a cysteine (Cys146). In addition to coordinating Mg^{2+}, this Asn is known to position an essential aspartate of the catalytic loop (22,23). We hypothesized that amino acid changes at these two positions are responsible for the loss of Mg^{2+}-binding by CASK, following the initial merger of a Mg^{2+}-coordinating CaM-kinase domain with the MAGUK domains during evolution. To test this hypothesis, we converted Gly162 and Cys146 of CASK to the canonical Asp and Asn residues, respectively, and tested binding of the mutants to an ATP analog (TNP-ATP) in the absence and presence of Mg^{2+}. TNP-ATP becomes fluorescent when inserted into the hydrophobic ATP-binding pocket of protein kinases (24). However, neither the single Gly162Asp or Cys146Asn mutants nor the double mutant conferred Mg^{2+}-TNP-ATP binding onto CASK (Figure 1).

Upon further sequence analysis, we observed two additional deviations from canonical CaM-kinases in residues that line the nucleotide-binding pocket of CASK, and could affect Mg^{2+}-ATP binding. First, Pro22 (which corresponds to a conserved alanine in standard CaM-kinases) could stiffen the Gly-rich loop of CASK, which as a consequence may lack sufficient flexibility to accommodate the Mg^{2+}-ATP complex. Moreover, Pro22 is unable to form a hydrogen bond with ATP phosphates, as it lacks a backbone NH group. Second, His145 in CASK replaces a negatively charged glutamate in the catalytic loop of standard CaM-kinases immediately preceding the Mg^{2+}-coordinating Asn.

To examine whether these additional changes in conserved residues contribute to the loss of Mg^{2+}-coordination in CASK, we reverted Pro22 and His145 to the canonical Ala and Glu residues, respectively, in addition to the initial Gly162Asp and Cys146Asn mutations. A CASK mutant containing Gly162Asp, Cys146Asn, and Pro22Ala was still incapable of coordinating TNP-ATP in the presence of Mg^{2+} (Figure 1). Only the quadruple mutant containing Gly162Asp, Cys146Asn, Pro22Ala and His145Glu, which we termed $CASK^{4M}$, displayed TNP-ATP binding in the presence of Mg^{2+} (Figure 1). The increase in fluorescence upon interaction of TNP-ATP with the $CASK^{4M}$ CaM-kinase domain was completely inhibited in the presence of excess ATP, indicating that TNP-ATP specifically mimics ATP (Supplemental Figure S1A).

Comparison of the catalytic properties of $CASK^{WT}$ and $CASK^{4M}$

ATP binding of $CASK^{4M}$ in the presence of Mg^{2+} suggested that it may behave catalytically like a conventional, Mg^{2+}-dependent CaM-kinase. To test this notion, we probed CASK mutants for kinase activity in the presence of Mg^{2+}-ATP and excess autocamtide-2 (a synthetic peptide substrate for CaMKII). Consistent with the results from Mg^{2+}-ATP binding, only the quadruple $CASK^{4M}$ mutant exhibited ATP-consumption in the presence of Mg^{2+} and substrate (Figure 2A) and an increase in autophosphorylation in presence of Mg^{2+}

(about threefold increase under saturating conditions; Figure 2B; about 30-fold increase under limiting conditions compared to the reactions without Mg^{2+}; Supplemental Figure S2A). Interestingly, all CASK mutants, including $CASK^{4M}$, still bound to ATP (Figure 1) and autophosphorylated (Figure 2B) in the absence of Mg^{2+}, retaining a unique activity of CASK not present in canonical CaM-kinases. Thus, $CASK^{4M}$ appears to bridge the Mg^{2+}-stimulated activity of classical CaM-kinases and the Mg^{2+}-independent activity of $CASK^{WT}$. It, therefore, represents a valuable tool to decipher the catalytic roles of the divalent metal ions in kinase reactions.

Mg^{2+} enhances the catalytic efficiency of $CASK^{4M}$

Various functions have been suggested for Mg^{2+} in kinase catalysis, including nucleotide binding, association and/or dissociation of the substrate peptide, and stabilization of the phosphotransfer transition state (22,25,26,27). To clarify the contribution of Mg^{2+} to phosphotransfer catalysis, we first tested whether the Mg^{2+} coordinating ability of $CASK^{4M}$ alters ATP binding (represented by interaction with the analog TNP-ATP).

TNP-ATP binding to $CASK^{4M}$ was similar with or without Mg^{2+} (Figure 2C) and similar to that of $CASK^{WT}$ without Mg^{2+} (Supplemental Figure S3A). However, ATP competed with TNP-ATP for binding to $CASK^{4M}$ better in the presence of Mg^{2+}, indicating that Mg^{2+} alters the affinity of ATP to $CASK^{4M}$ (Supplemental Figure S3B). We surmise that the effect of Mg^{2+} on ATP affinity is comparatively small; as it is masked in direct TNP-ATP affinity measurements, perhaps by additional contacts of the ATP analog. We also examined the enzymatic parameters of $CASK^{4M}$-mediated phosphotransfer in the absence and presence of Mg^{2+}. Efficient autophosphorylation was achieved in the presence of Mg^{2+} (Supplemental Figure S4). Moreover, catalysis, as measured by phosphate transferred onto autocamtide-2 by $CASK^{4M}$ was robustly enhanced by Mg^{2+} (Figure 2D). It is unlikely that the strong enhancement of catalytic efficiency of $CASK^{4M}$ in the presence of Mg^{2+} is due to the mild effect of Mg^{2+} on the nucleotide affinity we observed (see above). Therefore, our results suggest additional roles for Mg^{2+} downstream of ATP binding.

Overall structural comparison of $CASK^{WT}$, $CASK^{4M}$ and CaMKII

In order to trace the sources of the mechanistic differences in $CASK^{WT}$, $CASK^{4M}$ and CaMKII, we conducted crystal structure analyses. We crystallized the CaM-kinase domain of $CASK^{4M}$ under similar conditions as the CaM-kinase domain of $CASK^{WT}$, and solved the structure by molecular replacement at 2.0 Å resolution (Table 1). The $CASK^{4M}$ CaM-kinase domain exhibits a typical protein kinase fold, with an N-terminal lobe dominated by a five-stranded β-sheet and a primarily α-helical C-terminal lobe (Figure 3A). The C-terminal lobe is followed by a loop (residues 286-288) and an α-helix, αR1 (residues 289-303; Figure 3A, B), which are not part of the canonical kinase core. The overall structure of $CASK^{4M}$ CaM-kinase domain is significantly closer to that of $CASK^{WT}$ (PDB IDs 3C0G and 3C0I; RMSD 0.43-0.61 Å for 302 matching Cα atoms; (21)) than to that of CaMKII crystallized in an autoinhibited conformation (PDB ID 2BDW; RMSD 1.47-1.95 Å for 260-276 matching Cα atoms; (28)) (Figure 3A-C). Therefore, the four amino acid substitutions that confer Mg^{2+}-stimulated kinase activity onto $CASK^{4M}$ do not alter the overall structure of the CaM-kinase domain.

Divalent metal ions alter the positioning of the ATP phosphate moieties

To investigate the presumed additional role of Mg^{2+} beyond nucleotide binding, we determined the crystal structures of $CASK^{4M}$ in complex with either Na^{+}-AMPPNP or Mn^{2+}-AMPPNP (Table 1). AMPPNP is a non-hydrolyzable analog of ATP. Mn^{2+} is considered a stereochemical equivalent of Mg^{2+} (22,23). Consistent with the TNP-ATP binding data (Figures 1and 2C), $CASK^{4M}$ coordinated AMPPNP even in the absence of

divalent metal ions (Figure 4A). Conversely, after soaking CASK^{4M} crystals with Mn^{2+} solution, we failed to discern a bound divalent ion in the absence of AMPPNP (Supplemental Figure S5A), suggesting that Mg^{2+} is coordinated only when complexed with the nucleotide.

The overall orientation of the adenosine moiety of AMPPNP was similar in the presence or absence of Mn^{2+} (Figure 4A, B) and AMPPNP could be modeled in a similar orientation into the nucleotide-binding pocket of CASK^{WT} without steric clashes, suggesting that the global positioning of ATP and the orientation of the base moiety is not affected by the divalent cation. However, the orientation of β- and γ-phosphates of AMPPNP was specifically altered by Mn^{2+} in CASK^{4M} (Figure 4A, B). We therefore conclude that Mg^{2+} positions the phosphates of ATP in the nucleotide-binding pocket of CASK^{4M} independent of the positioning of the adenosine moiety, which is consistent with previous studies on PKA (29,30).

Role of Mg^{2+} in kinase catalysis

Kinases vary in the manner by which Mg^{2+} ions bind the ATP phosphates in their active sites (22,31). In order to unequivocally locate divalent metal ion(s) in the Mn^{2+}-AMPPNP complex of CASK^{4M} CaM-kinase domain, we measured diffraction at an X-ray wavelength of 1.88 Å, where Mn^{2+} exhibits a measurable anomalous signal, and calculated anomalous difference Fourier maps. This procedure unequivocally revealed a single coordinated Mn^{2+} ion in the Mn^{2+}-AMPPNP co-crystal structure of CASK^{4M} CaM-kinase domain (Figure 4C).

Similar to some conventional kinases, such as DAPKI and MEK1, (32,33) the Mn^{2+} ion in the CASK^{4M} CaM-kinase domain, coordinates the β-phosphate and indirectly orients the γ-phosphate in a puppet-master fashion (Figure 4C). Therefore, we surmise that the role of Mg^{2+} in enhancing kinase catalysis is to position the γ-phosphate in proximity of the conserved Lys41, as well as to stabilize the transition state. Mg^{2+} may also enhance the leaving group properties of ADP by compensating for additional negative charge that evolves at the β-phosphate during the reaction. Taken together, our observations are consistent with the notion that Mg^{2+} coordinates the ATP phosphates to favor a catalytically productive kinase-ATP complex (22,25,23,34,35).

His145 may act as a Mg^{2+} sensor in CASK^{WT}

The conformation of residues lining the ATP-binding pockets of the CASK^{4M} (this work) and CASK^{WT} (21) kinase domains are very similar. Differences are strictly limited to the four amino acid exchanges. Ala22 and Asn146 in CASK^{4M} adopt very similar conformations as the corresponding Pro22 and Cys146 in CASK^{WT}. Apart from the introduction of the Asp162 side chain (instead of Gly162 in CASK^{WT}), the most pronounced difference is a change in side chain orientation of Glu145 in CASK^{4M} compared to the corresponding His145 in CASK^{WT} (compare Figure 4A with D). In CASK^{WT}, His145 protrudes into the nucleotide-binding pocket (Figure 4D) and spatially overlaps with a water molecule in the coordination sphere of the Mn^{2+} ion bound in the CASK^{4M}-Mn^{2+}-AMPPNP co-crystal structure (Figure 4B, C). In CASK^{4M}, Glu145 is sequestered by Arg302 from the C-terminal extension and is thereby turned away from the ATP pocket (Figure 4A, B and Supplemental Figure S5A, B). A similar situation is seen in CaMKII (28). Since the triple mutant Gly162Asp/Cys146Asn/Pro22Ala of CASK is still inhibited by Mg^{2+} (Figure 2B), these observations suggest that His145 is not tolerated in the coordination sphere of the divalent metal ion. TNP-ATP binding to CASK^{WT} is partially inhibited by Mg^{2+} at pH 8.8, where most His side chains are expected to be neutral (Supplemental Figure S1B). However, the local pH is difficult to estimate and His145 may still be protonated within the CASK^{WT}

ATP-binding pocket. Thus, our data suggest that His145 does not allow metal coordination in $CASK^{WT}$ by invading the coordination sphere of the in-coming metal ion.

Additional features supporting the Mg^{2+}-independent activities of $CASK^{WT}$ and $CASK^{4M}$

Although the phosphorylation activity of the $CASK^{4M}$ CaM-kinase domain is strongly stimulated by Mg^{2+}, the enzyme still exhibits catalytic activity in the absence of Mg^{2+} (Figure 2B). Similarly, $CASK^{WT}$ binds ATP and performs phosphotransfer in the absence of Mg^{2+} (21). Therefore, CASK must have undergone evolutionary adaptions, which are retained in $CASK^{4M}$ and which allow catalysis without Mg^{2+}. As one possibility, CASK may have acquired features that promote the kinase-ATP-substrate ternary complex formation and elevate substrate phosphorylation under chemically sub-optimal conditions (i.e. in the absence of Mg^{2+}).

Both $CASK^{WT}$ (21) and $CASK^{4M}$ CaM-kinase domains retained bound nucleotide during purification and crystallization in the absence of added nucleotides (Figure 4D and Supplemental Figure S5B), unlike other constitutively active kinases such as casein kinase II and PIM1, which are purified in their apo-forms (36,37). We modeled this nucleotide as an adenosine-3′-phosphate molecule (3′-AMP), likely a product of bacterial RNA degradation during cell rupture. The binding mode of 3′-AMP clearly differs from the binding of AMPPNP in either enzyme (compare Figure 4A, B with Figure 4D and Supplemental Figure S5B), and 3′-AMP is easily detached from the pocket since no residual electron density was discerned in the nucleotide-binding pocket of $CASK^{4M}$ after washing of the crystals in Mn^{2+}-containing buffer (see above; Supplemental Figure S5A). Nevertheless, co-purification of the nucleotide attests the general accessibility of the nucleotide-binding pockets of $CASK^{WT}$ and $CASK^{4M}$. These observations indirectly support the idea that $CASK^{WT}$ and $CASK^{4M}$ adopt a nucleotide-receptive fold that ensures an unregulated occupancy of their nucleotide-binding pockets by ATP even in the absence of Mg^{2+}. A constitutive supply of ATP may partly compensate for the inability of $CASK^{WT}$ to utilize the co-factor Mg^{2+}.

Features supporting the Ca^{2+}-independent activities of $CASK^{WT}$ and $CASK^{4M}$

In their active states, protein kinases adopt a conserved conformation of the two lobes, in which their functional elements are poised for substrate binding and catalysis (3,38). By default, archetypical CaM-kinases adopt autoinhibited conformations (39,28). The activation of CaM-kinases requires binding of Ca^{2+}/CaM to the autoregulatory domain leading to their detachment from the kinase domain and restoration of the active conformation. Therefore, Ca^{2+} is required for optimal catalysis by CaM-kinases (39,28).

Immediately following the kinase domain, CASK contains a sequence homologous to the autoregulatory domain of CaMKII (residues 281-310) which binds to Ca^{2+}/CaM (10). Similar to CaMKI and CaMKII, residues 289-302 of CASK form a helical extension (αR1) which packs against the C-terminal lobe (Figure 3 and Supplemental Figure S6). However, neither in $CASK^{WT}$ (21) nor in $CASK^{4M}$, helix αR1 or its C-terminal extension engages in direct contacts with residues of the ATP-binding cleft (Figure 3A)(39). Also, CASK displays an arginine to leucine substitution in the RXXT/S motif of its autoregulatory domain. A similar mutation in the CaMKII autoinhibitory segment can reduce the affinity of the autoinhibitory segment to the substrate-binding site by up to 200-fold (40,41). As a consequence, the $CASK^{WT}$ and $CASK^{4M}$ CaM-kinase domains, including the putative autoinhibitory regions, remain compatible with constitutive substrate binding. This allows increased formation of the ternary kinase-ATP-substrate complexes, which partly compensates for the failure of $CASK^{WT}$ to utilize Mg^{2+}.

Since $CASK^{4M}$ is not inhibited by divalent ions, we were able to directly test the effect of Ca^{2+}/CaM on the rate of catalysis. We first measured the Mg^{2+}-stimulated catalytic kinetics of $CASK^{4M}$ towards autocamtide-2 (a CaMKII specific substrate) in absence of Ca^{2+}/CaM. Under these conditions, $CASK^{4M}$ has a maximum velocity of ≈ 1 μmol/μmol/min and Michaelis constant for ATP is ≈ 70 μM (Figure 5A). These parameters are comparable with those of Ca^{2+}/Calmodulin-activated CaMKIV for Synapsin I (also a CAMKII substrate) (42). Importantly, addition of Ca^{2+}/CaM had no stimulating effect on the kinase activity of $CASK^{4M}$ (Figure 5B). Together, the structural and the enzymological data suggest that CASK retains a non-functional autoinhibitory domain, possibly as an evolutionary vestige of its CaM-kinase ancestors. Correspondingly, both $CASK^{WT}$ and $CASK^{4M}$ exhibited autophosphorylation activity in complete absence of divalent ions, unlike CaMKII (Supplemental Figure S2C). Whether Ca^{2+}/CaM binding to CASK has another physiological role remains to be tested.

$CASK^{WT}$ and $CASK^{4M}$ show similar intracellular kinase activities

The $CASK^{4M}$ activity was stimulated by Mg^{2+} and was considerably higher than the activity of $CASK^{WT}$ in the presence or absence of Mg^{2+} *in vitro* (Figure 2B, D and Supplemental Figures S2A, B). In cells, the majority of ATP is bound to Mg^{2+}. We therefore asked whether in a cytosolic milieu, full-length $CASK^{4M}$ would also yield higher levels of phosphorylated target compared to full-length $CASK^{WT}$. Apart from CASK itself, neurexin-1 is presently the only characterized *in vivo* substrate of CASK (21). Neurexin-1 was co-transfected with full-length $CASK^{WT}$ and $CASK^{4M}$ into HEK 293T cells, and the steady-state phosphorylation status of neurexin-1 was quantified (Figure 5C, D). As a control, we used $tCASK^{WT}$, in which amino acids 1-161 have been deleted, thus severely truncating the kinase domain but leaving the MAGUK domains intact. Surprisingly, neither autophosphorylation nor neurexin-1 phoshorylation levels at steady state level were significantly augmented in $CASK^{4M}$ compared to $CASK^{WT}$ (Figure 5C, D). Thus in the cytosol, CASK activity seems sufficient for maximum neurexin-1 phosphorylation. Most likely, the PDZ domain of CASK, which binds neurexin-1 (10), ensures a constant supply of substrate (21).

Based on the above observations, we suggest that the MAGUK scaffolding domains of CASK spatially constrain the CASK kinase activity to the vicinity of the membrane-bound cell adhesion protein complexes, to which CASK binds. This scaffolding interaction not only raises the local substrate concentration and specificity, but also sustains stoichiometry between CASK and its substrate.

Evolution of CASK from a Mg^{2+}-coordinating kinase

The inability of Mg^{2+}-coordinating $CASK^{4M}$ to increase neurexin-1 phosphorylation in a cellular environment raises the possibility that the original CaM-kinase domain, which merged with a MAGUK to give rise to an ancestral CASK kinase, could have been a canonical Mg^{2+}-coordinating enzyme. Thus, we searched for CASK-like sequences in evolutionarily ancient metazoan and animal species (Supplemental Figure S7).

We detected the most ancient CASK proteins in metazoans that characterize the emergence of animals in evolution. A CASK ortholog was detected in the placozoan *Trichoplax adherens*, (Figure 6B) which lacks tissue differentiation but contains multiple neuronal proteins (43). Placozoan CASK exhibits canonical residues at three of the four positions, we investigated herein as a source of Mg^{2+}-sensitivity in vertebrate CASK; at the 145-equivalent position in the catalytic loop, where vertebrate CASK carries a histidine instead of a glutamate, placozoan CASK features a glutamine. A similar Glu-to-Gln exchange is found in some active human CaM-kinases, e.g. DRAK-1 or -2, and is therefore compatible

with a canonical Mg^{2+}-dependent kinase mechanism. Thus, placozoan CASK resembles $CASK^{4M}$ and may represent a Mg^{2+}-stimulated evolutionary CASK relic.

Cnidarians like *Nematostella vectensis*, the sea anemone, contain differentiated tissues, including neuronal tissue. The CASK ortholog of the sea anemone exhibits a single Glu to His substitution in the catalytic loop (Figure 6A). Our CASK triple mutant (Gly162Asp/Cys146Asn/Pro22Ala), which is not stimulated by Mg^{2+} (Figure 1) is most similar to the Cnidarian CASK.

All four of the amino acid changes we have investigated herein first appear together in the subkingdom bilateria, as seen in platyhelminthes (*Schistosoma japonicum*), and are conserved thereafter. Curiously, ecdysozoans (moulting animals) like nematodes (*Caenorhabditis elegans*) and arthropods (*Drosophila melanogaster*) exhibit sporadic variations in these substitutions (Figure 6A), whose functional implications remain to be investigated.

Taken together, our phylogenetic analysis indicates that CASK arose from the fusion of a Mg^{2+}-coordinating CaM-kinase domain with a membrane palmitoylated protein (MPP)-like scaffolding MAGUK. This fusion happened concurrently with the development of the basal metazoans. The substrate-scaffolding function provided by the MAGUK domains then could have allowed CASK to gradually shed its dependence on Mg^{2+}. These changes rendered CASK completely dependent on substrate recruitment *via* its MAGUK domains, such as on the PDZ-domain-dependent binding of neurexins.

DISCUSSION

Mammals contain at least 22 MAGUK proteins that vary in size and domain structure (44). MAGUKs are absent from bacterial, plant, fungal and protozoan genomes, suggesting that their evolution coincides with the emergence of animals. CASK, the only MAGUK bearing a CaM-kinase domain at its N-terminus, first appeared evolutionarily either simultaneous to, or shortly after, the emergence of MAGUKs in basal metazoans. Mutations in CASK are associated with numerous human developmental anomalies (16,17,18,19,20,45) and the *CASK* gene is essential in mice (15). Although CASK was considered a pseudokinase due to its lack of Mg^{2+}-binding (8,1), we recently found that CASK is an active kinase, and represents the first known kinase inhibited by Mg^{2+}, a co-factor of conventional kinases (21). In the present study, we examined the structural mechanism that confers onto CASK its unique Mg^{2+}-sensitivity. We identified four evolutionarily conserved residues that determine this property, and show that mutation of these residues converts Mg^{2+}-inhibition of CASK into Mg^{2+}-stimulation.

Pseudokinases constitute 10 % of the human kinome. Many pseudokinases perform critical cellular functions, although prior to the identification of kinase activity in CASK, no pseudokinase was shown to be catalytically active. Moreover, prior to the current study, back mutation attempts to convert pseudokinases into standard kinases had failed, possibly due to incomplete understanding of the precise evolutionary changes involved (46,47). Indeed, there are other pseudokinases (such as the Trb-family of Ser/Thr kinases, and CCK4 tyrosine kinase) with substitutions in the Mg^{2+}-binding motifs analogous to those observed in CASK (8), and it is possible that these other pseudokinases may also be catalytically active under defined conditions. The mutations described here for $CASK^{4M}$ may also convert these other enzymes into Mg^{2+}-dependent kinases. Thus, similar to CASK, these atypical kinase domains may have accumulated changes, which specialize them for a particular physiological niche.

Mg^{2+} has been postulated to promote kinase catalysis in multiple ways, including nucleotide binding, γ-phosphate positioning and stabilization of the transition state. Our ability to generate a Mg^{2+}-coordinating mutant of CASK, $CASK^{4M}$, in which Mg^{2+} strongly accelerated phosphotransfer, allowed us to directly address the mechanisms of Mg^{2+}-dependent catalytic enhancement. Analysis of crystal structures together with enzymatic studies strongly suggested that Mg^{2+} acts primarily downstream of ATP binding, and positions the γ-phosphate of bound ATP optimally for catalysis by binding to its ß-phosphate. In addition, direct binding to the ß-phosphate suggests that stabilization of the transition state and compensation of the additional negative charge evolving at the ß-phosphate during phosphate transfer (thus enhancing the property of ADP as a leaving group) are also possible roles of Mg^{2+} during catalysis.

Phylogenetically, the CASK CaM-kinase domain falls near the CaMKII cluster (1), whose members are autoinhibited by a Ca^{2+}/CaM dependent regulatory domain (28). Yet, unlike CaMKII, a Arg-to-Leu substitution that is seen even in the most primitive placozoan CASK leaves its autoregulatory segment suboptimal for competing with substrate binding. Moreover, unlike CaMKII (28), CASK exhibits no dimerization of the autoregulatory domain and constitutively adopts an active, closed conformation. This conformation permits uninterrupted ATP-binding to the nucleotide-binding pocket of CASK possibly in part compensating for the suboptimal, Mg^{2+}-independent phosphotransfer chemistry that the enzyme employs.

Moreover, the merger of an ancestral CASK kinase domain with a MAGUK linked the enzyme activity to the MAGUK scaffolding domains, which could recruit its substrate, thereby a) facilitating phosphotransfer by increasing the local substrate-concentration, b) increasing substrate-specificity (9) and c) eliminating the need for fast catalytic turnover (Figure 6C). Based on the above features, CASK enjoys continuous access to both ATP and its protein substrate, rendering the enzyme independent of both Mg^{2+} and Ca^{2+}.

The presence of Mg^{2+}-coordinating residues in placozoan CASK suggests that the lack of stimulation of CASK by Mg^{2+} was acquired following, and possibly as a result of, its independence from divalent ions. The primary change in this direction seems to be the acquisition of a His145-equivalent in the nucleotide-binding pocket, which appears to be critical to counteract Mg^{2+} coordination. This change may have caused a lack of evolutionary pressure to maintain a flexible glycine-rich (GR) loop or Mg^{2+}-coordinating residues elsewhere in the domain, thus inviting secondary changes in the nucleotide-binding pocket. Once optimized over the evolutionary time scale, this domain architecture was maintained in all Chordates.

Why was CASK transformed from a putative Mg^{2+}-stimulated to a Mg^{2+}-inhibited kinase early in evolution? One possibility is that Mg^{2+} was simply unnecessary in the context of the substrate recruiting mechanism implemented by the MAGUK domains of CASK (21). Consistent with this idea, our experiments in cells (Figure 5C) demonstrate that Mg^{2+}-stimulation does not confer increased steady state phosphorylation in a cellular context when the substrate is recruited by the PDZ-domain. An additional possibility is that divalent ion-sensitivity evolved with emergence of excitable cells like those in the nervous tissue, as a mechanism of negative regulation. Localized influx of divalent ions might significantly reduce the free ATP concentration at a synapse, thereby negatively regulating the catalytic rate of CASK (Figure 6C). Taken together, it appears that the multi-domain structure of CASK allowed the CaM-kinase domain to shed its Mg^{2+} dependence, which led to evolution of CASK into a hybrid kinase, exhibiting a substrate recruitment module (PDZ domain) fused to a slow, regulated catalytic module (CaM-kinase domain).

Supplementary Material

Refer to Web version on PubMed Central for supplementary material.

Acknowledgments

We thank members of the Südhof and Jahn laboratories for discussions and Reinhard Lührmann for providing generous access to crystallography equipment. We are grateful to the support by the staff of beamline BL14.2 (BESSY, Berlin, Germany) for help during diffraction data collection. This work was supported by a grant from the NIMH (R37 MH52804-08 to TCS) and the Max-Planck-Society. MS is a Human Frontiers Long Term Fellow.

REFERENCES

1. Manning G, Whyte DB, Martinez R, Hunter T, Sudarsanam S. The protein kinase complement of the human genome. Science. 2002; 298:1912–34. [PubMed: 12471243]
2. Noble ME, Endicott JA, Johnson LN. Protein kinase inhibitors: insights into drug design from structure. Science. 2004; 303:1800–5. [PubMed: 15031492]
3. Huse M, Kuriyan J. The conformational plasticity of protein kinases. Cell. 2002; 109:275–82. [PubMed: 12015977]
4. Hanks SK, Quinn AM, Hunter T. The protein kinase family: conserved features and deduced phylogeny of the catalytic domains. Science. 1988; 241:42–52. [PubMed: 3291115]
5. Taylor SS, Radzio-Andzelm E. Three protein kinase structures define a common motif. Structure. 1994; 2:345–55. [PubMed: 8081750]
6. Higgins JM. Haspin-like proteins: a new family of evolutionarily conserved putative eukaryotic protein kinases. Protein Sci. 2001; 10:1677–84. [PubMed: 11468364]
7. Mayans O, van der Ven PF, Wilm M, Mues A, Young P, Furst DO, Wilmanns M, Gautel M. Structural basis for activation of the titin kinase domain during myofibrillogenesis. Nature. 1998; 395:863–9. [PubMed: 9804419]
8. Boudeau J, Miranda-Saavedra D, Barton GJ, Alessi DR. Emerging roles of pseudokinases. Trends Cell Biol. 2006
9. Ubersax JA, Ferrell JE Jr. Mechanisms of specificity in protein phosphorylation. Nat Rev Mol Cell Biol. 2007; 8:530–41. [PubMed: 17585314]
10. Hata Y, Butz S, Sudhof TC. CASK: a novel dlg/PSD95 homolog with an N-terminal calmodulin-dependent protein kinase domain identified by interaction with neurexins. J Neurosci. 1996; 16:2488–94. [PubMed: 8786425]
11. Cohen AR, Woods DF, Marfatia SM, Walther Z, Chishti AH, Anderson JM. Human CASK/LIN-2 binds syndecan-2 and protein 4.1 and localizes to the basolateral membrane of epithelial cells. J Cell Biol. 1998; 142:129–38. [PubMed: 9660868]
12. Hsueh YP, Wang TF, Yang FC, Sheng M. Nuclear translocation and transcription regulation by the membrane-associated guanylate kinase CASK/LIN-2. Nature. 2000; 404:298–302. [PubMed: 10749215]
13. Hsueh YP, Yang FC, Kharazia V, Naisbitt S, Cohen AR, Weinberg RJ, Sheng M. Direct interaction of CASK/LIN-2 and syndecan heparan sulfate proteoglycan and their overlapping distribution in neuronal synapses. J Cell Biol. 1998; 142:139–51. [PubMed: 9660869]
14. Biederer T, Sara Y, Mozhayeva M, Atasoy D, Liu X, Kavalali ET, Sudhof TC. SynCAM, a synaptic adhesion molecule that drives synapse assembly. Science. 2002; 297:1525–31. [PubMed: 12202822]
15. Atasoy D, Schoch S, Ho A, Nadasy KA, Liu X, Zhang W, Mukherjee K, Nosyreva ED, Fernandez-Chacon R, Missler M, Kavalali ET, Sudhof TC. Deletion of CASK in mice is lethal and impairs synaptic function. Proc Natl Acad Sci U S A. 2007; 104:2525–30. [PubMed: 17287346]
16. Dimitratos SD, Stathakis DG, Nelson CA, Woods DF, Bryant PJ. The location of human CASK at Xp11.4 identifies this gene as a candidate for X-linked optic atrophy. Genomics. 1998; 51:308–9. [PubMed: 9722958]
17. Froyen G, Van Esch H, Bauters M, Hollanders K, Frints SG, Vermeesch JR, Devriendt K, Fryns JP, Marynen P. Detection of genomic copy number changes in patients with idiopathic mental

retardation by high-resolution X-array-CGH: important role for increased gene dosage of XLMR genes. Hum Mutat. 2007; 28:1034–42. [PubMed: 17546640]

18. Hayashi S, Mizuno S, Migita O, Okuyama T, Makita Y, Hata A, Imoto I, Inazawa J. The CASK gene harbored in a deletion detected by array-CGH as a potential candidate for a gene causative of X-linked dominant mental retardation. Am J Med Genet A. 2008; 146A:2145–51. [PubMed: 18629876]
19. Najm J, Horn D, Wimplinger I, Golden JA, Chizhikov VV, Sudi J, Christian SL, Ullmann R, Kuechler A, Haas CA, Flubacher A, Charnas LR, Uyanik G, Frank U, Klopocki E, Dobyns WB, Kutsche K. Mutations of CASK cause an X-linked brain malformation phenotype with microcephaly and hypoplasia of the brainstem and cerebellum. Nat Genet. 2008
20. Samuels BA, Hsueh YP, Shu T, Liang H, Tseng HC, Hong CJ, Su SC, Volker J, Neve RL, Yue DT, Tsai LH. Cdk5 promotes synaptogenesis by regulating the subcellular distribution of the MAGUK family member CASK. Neuron. 2007; 56:823–37. [PubMed: 18054859]
21. Mukherjee K, Sharma M, Urlaub H, Bourenkov GP, Jahn R, Sudhof TC, Wahl MC. CASK Functions as a Mg2+-independent neurexin kinase. Cell. 2008; 133:328–39. [PubMed: 18423203]
22. Adams JA. Kinetic and catalytic mechanisms of protein kinases. Chem Rev. 2001; 101:2271–90. [PubMed: 11749373]
23. Hanks SK, Hunter T. Protein kinases 6. The eukaryotic protein kinase superfamily: kinase (catalytic) domain structure and classification. Faseb J. 1995; 9:576–96. [PubMed: 7768349]
24. Stewart RC, VanBruggen R, Ellefson DD, Wolfe AJ. TNP-ATP and TNP-ADP as probes of the nucleotide binding site of CheA, the histidine protein kinase in the chemotaxis signal transduction pathway of Escherichia coli. Biochemistry. 1998; 37:12269–79. [PubMed: 9724541]
25. Adams JA, Taylor SS. Divalent metal ions influence catalysis and active-site accessibility in the cAMP-dependent protein kinase. Protein Sci. 1993; 2:2177–86. [PubMed: 8298463]
26. Cheng Y, Zhang Y, McCammon JA. How does the cAMP-dependent protein kinase catalyze the phosphorylation reaction: an ab initio QM/MM study. J Am Chem Soc. 2005; 127:1553–62. [PubMed: 15686389]
27. Saylor P, Wang C, Hirai TJ, Adams JA. A second magnesium ion is critical for ATP binding in the kinase domain of the oncoprotein v-Fps. Biochemistry. 1998; 37:12624–30. [PubMed: 9730835]
28. Rosenberg OS, Deindl S, Sung RJ, Nairn AC, Kuriyan J. Structure of the autoinhibited kinase domain of CaMKII and SAXS analysis of the holoenzyme. Cell. 2005; 123:849–60. [PubMed: 16325579]
29. Herberg FW, Doyle ML, Cox S, Taylor SS. Dissection of the nucleotide and metal-phosphate binding sites in cAMP-dependent protein kinase. Biochemistry. 1999; 38:6352–60. [PubMed: 10320366]
30. Narayana N, Cox S, Nguyen-huu X, Ten Eyck LF, Taylor SS. A binary complex of the catalytic subunit of cAMP-dependent protein kinase and adenosine further defines conformational flexibility. Structure. 1997; 5:921–35. [PubMed: 9261084]
31. Waas WF, Rainey MA, Szafranska AE, Cox K, Dalby KN. A kinetic approach towards understanding substrate interactions and the catalytic mechanism of the serine/threonine protein kinase ERK2: identifying a potential regulatory role for divalent magnesium. Biochim Biophys Acta. 2004; 1697:81–7. [PubMed: 15023352]
32. Ohren JF, Chen H, Pavlovsky A, Whitehead C, Zhang E, Kuffa P, Yan C, McConnell P, Spessard C, Banotai C, Mueller WT, Delaney A, Omer C, Sebolt-Leopold J, Dudley DT, Leung IK, Flamme C, Warmus J, Kaufman M, Barrett S, Tecle H, Hasemann CA. Structures of human MAP kinase kinase 1 (MEK1) and MEK2 describe novel noncompetitive kinase inhibition. Nat Struct Mol Biol. 2004; 11:1192–7. [PubMed: 15543157]
33. Tereshko V, Teplova M, Brunzelle J, Watterson DM, Egli M. Crystal structures of the catalytic domain of human protein kinase associated with apoptosis and tumor suppression. Nat Struct Biol. 2001; 8:899–907. [PubMed: 11573098]
34. Niefind K, Guerra B, Ermakowa I, Issinger OG. Crystal structure of human protein kinase CK2: insights into basic properties of the CK2 holoenzyme. Embo J. 2001; 20:5320–31. [PubMed: 11574463]

35. Valiev M, Yang J, Adams JA, Taylor SS, Weare JH. Phosphorylation reaction in cAPK protein kinase-free energy quantum mechanical/molecular mechanics simulations. J Phys Chem B. 2007; 111:13455–64. [PubMed: 17983217]
36. Battistutta R, De Moliner E, Sarno S, Zanotti G, Pinna LA. Structural features underlying selective inhibition of protein kinase CK2 by ATP site-directed tetrabromo-2- benzotriazole. Protein Sci. 2001; 10:2200–6. [PubMed: 11604527]
37. Qian KC, Wang L, Hickey ER, Studts J, Barringer K, Peng C, Kronkaitis A, Li J, White A, Mische S, Farmer B. Structural basis of constitutive activity and a unique nucleotide binding mode of human Pim-1 kinase. J Biol Chem. 2005; 280:6130–7. [PubMed: 15525646]
38. Nolen B, Taylor S, Ghosh G. Regulation of protein kinases; controlling activity through activation segment conformation. Mol Cell. 2004; 15:661–75. [PubMed: 15350212]
39. Goldberg J, Nairn AC, Kuriyan J. Structural basis for the autoinhibition of calcium/calmodulin-dependent protein kinase I. Cell. 1996; 84:875–87. [PubMed: 8601311]
40. Fong YL, Soderling TR. Studies on the regulatory domain of Ca2+/calmodulin-dependent protein kinase II. Functional analyses of arginine 283 using synthetic inhibitory peptides and site-directed mutagenesis of the alpha subunit. J Biol Chem. 1990; 265:11091–7. [PubMed: 1972705]
41. Smith MK, Colbran RJ, Brickey DA, Soderling TR. Functional determinants in the autoinhibitory domain of calcium/calmodulin-dependent protein kinase II. Role of His 282 and multiple basic residues. J Biol Chem. 1992; 267:1761–8. [PubMed: 1309796]
42. Miyano O, Kameshita I, Fujisawa H. Purification and characterization of a brain-specific multifunctional calmodulin-dependent protein kinase from rat cerebellum. J Biol Chem. 1992; 267:1198–203. [PubMed: 1309765]
43. Srivastava M, Begovic E, Chapman J, Putnam NH, Hellsten U, Kawashima T, Kuo A, Mitros T, Salamov A, Carpenter ML, Signorovitch AY, Moreno MA, Kamm K, Grimwood J, Schmutz J, Shapiro H, Grigoriev IV, Buss LW, Schierwater B, Dellaporta SL, Rokhsar DS. The Trichoplax genome and the nature of placozoans. Nature. 2008; 454:955–60. [PubMed: 18719581]
44. te Velthuis AJ, Admiraal JF, Bagowski CP. Molecular evolution of the MAGUK family in metazoan genomes. BMC Evol Biol. 2007; 7:129. [PubMed: 17678554]
45. Wang Q, Lu J, Yang C, Wang X, Cheng L, Hu G, Sun Y, Zhang X, Wu M, Liu Z. CASK and its target gene Reelin were co-upregulated in human esophageal carcinoma. Cancer Lett. 2002; 179:71–7. [PubMed: 11880184]
46. Boudeau J, Scott JW, Resta N, Deak M, Kieloch A, Komander D, Hardie DG, Prescott AR, van Aalten DM, Alessi DR. Analysis of the LKB1-STRAD-MO25 complex. J Cell Sci. 2004; 117:6365–75. [PubMed: 15561763]
47. Prigent SA, Gullick WJ. Identification of c-erbB-3 binding sites for phosphatidylinositol 3′-kinase and SHC using an EGF receptor/c-erbB-3 chimera. Embo J. 1994; 13:2831–41. [PubMed: 8026468]

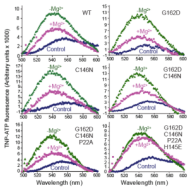

Figure 1. Designing a Mg^{2+}-coordinating version of CASK CaM-kinase domain

Fluorescence emission spectra of TNP-ATP in the presence of WT and mutant CASK. The protein analyzed (WT or mutant) is indicated in the upper right corner. Dark blue trace: Control spectrum of TNP-ATP (1 μM) in Tris-HCl buffer (pH 7.0) with EDTA (4 mM). Green trace: Spectra of samples containing 1 μM of the indicated recombinant CASK CaM-kinase domain, TNP-ATP (1 μM) and EDTA (4 mM) in Tris-HCl buffer (pH 7.0). Magenta trace: Spectra of samples containing 1 μM of the indicated recombinant CASK CaM-kinase domain, TNP-ATP (1 μM) and 100 μM $MgCl_2$ in Tris-HCl buffer (pH 7.0). Samples were excited at 410 nm, and spectra were recorded between 500 and 600 nm. The spectra are representatives of experiments repeated three times with essentially identical results.

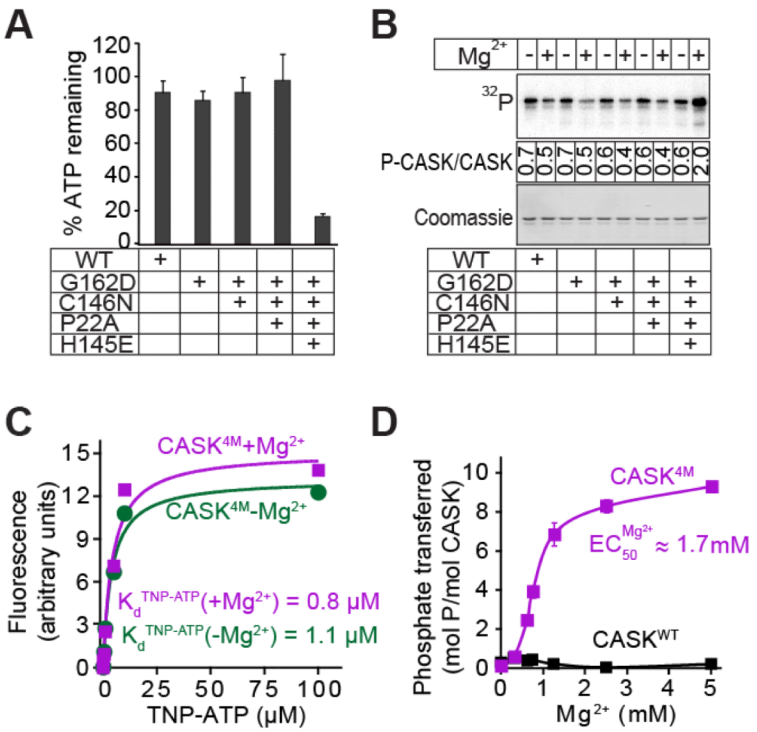

Figure 2. Effect of divalent ions on nucleotide-binding and hydrolysis

A. ATP consumption by WT or mutant CASK CaM-kinase domain. In Tris-HCl buffer (pH 7.0) supplemented with Ca^{2+} (1 mM), CaM (4 μM), and Mg^{2+} (2 mM), indicated variant of CASK CaM-kinase domain (1 μM), Autocamtide-2 (100 μM) and ATP (50 μM) were incubated for 60 min. The amount of ATP remaining was detected with KinaseGlo^{tm}. Data represents means ± standard deviation of three independent experiments.

B. Autophosphorylation of WT and mutant CASK CaM-kinase domains. The indicated variants of CASK CaM-kinase domain (1 μM) were incubated in Tris-HCl buffer (pH 7.0) with Na^{+}-γ^{32}P-ATP (50 cpm/pmol; -Mg^{2+}) or 10 mM Mg^{2+}-ATP (+Mg^{2+}) at 30°C with shaking for 2 h. The proteins were separated by SDS-PAGE, transferred onto a nitrocellulose membrane, and visualized by phosphorimager scanning (upper panel). Ponceau staining was used for loading control (lower panel). Mean stoichiometry of phosphate incorporation (phosphates/CASK molecule) from three independent experiments are shown between the panels.

C. TNP-ATP binding. Increasing amounts of TNP-ATP were added to cuvettes containing 10 mM Tris-HCl pH 7.0, 1 μM CASK^{4M}, and either 4 mM EDTA (magenta symbols) or 200 μM Mg^{2+} (green symbols). The TNP-ATP fluorescence of the samples (excitation: 410 nm; emission: 541 nm) is plotted after subtracting background TNP-ATP fluorescence obtained with parallel samples, which contained the same TNP-ATP, Tris-HCl, EDTA, or Mg^{2+} concentrations but lysozyme instead of CASK. The plot is a representative of three independent experiments.

D. Effect of Mg^{2+} on kinase activity of CASK^{4M}. Indicated variants of CASK CaM-kinase domain (2 μM), autocamtide-2 (100 μM) and γ^{32}P-ATP (250 μM; 250 cpm/pmol) in Tris-HCl buffer (pH 7.0) were incubated for 10 min with increasing amounts of Mg^{2+}. Amount of phospho-autocamtide-2 generated was estimated by scintillation counting of dot-blots on nitrocellulose membrane. Data shown are means ± standard errors of the means (SEMs; n=3).

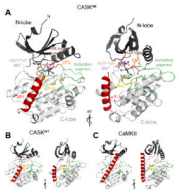

Figure 3. Overview of the CASK^{4M}-Mn^{2+}-AMPPNP crystal structure

A. Orthogonal ribbon plot of CASK^{4M} CaM-kinase domain with landmark functional elements colored. Gly-rich loop (GR-loop) - brown, catalytic loop (C-loop) - yellow; DFG motif of the Mg^{2+}-binding loop - orange; activation segment - green; C-terminal Ca^{2+}/CaM-binding element - red. AMPPNP and residues Asn146 and Asp162, which coordinate the Mn^{2+} ion, are shown as sticks and colored by atom type. Carbon - beige; oxygen - red; nitrogen - blue; phosphorus - pink. B. Structure of CASK CaM-kinase domain in complex with AMPPNP (sticks) lacking a divalent metal ion (β and γ phosphates disordered; pdb ID 3C0H; (21)) in the same orientation as the CASK^{4M} CaM-kinase domain in A. Cys146 is shown as sticks. Functional elements are colored as in A. C. Structure of CaMKII (pdb ID 2BDW; (28)) in the same orientation as the CASK^{4M} CaM-kinase domain in A. Asn140 and Asp156, whose equivalents in CASK^{4M} coordinate the Mn^{2+} ion, are shown as sticks. Functional elements are colored as in A.

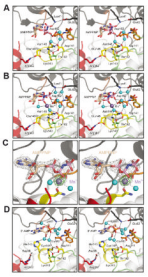

Figure 4. Nucleotide-binding pocket of the CASK^{4M} CaM-kinase domain

A. CASK^{4M} CaM-kinase in complex with AMPPNP without a divalent metal ion.

B. CASK^{4M} CaM-kinase in complex with AMPPNP-Mn^{2+}. Residues of the Mg^{2+}-binding loop are shown in orange, residues of the catalytic loop are in yellow and residues of the C-terminal Ca^{2+}/CaM-binding element are in red (as in Figure 3). Selected residues and the nucleotides are shown as sticks and colored by atom type; carbon - as the respective fragment; oxygen - red; nitrogen - blue; phosphorus - pink. Water molecules (cyan) and the Mn^{2+} ion (purple) are shown as spheres. The orientations are the same as in Figure 3A left panel. The orientations of the AMPPNP β and γ-phosphates differ in the complexes without and with Mn^{2+} (compare panels A and B).

C. Stereo plot showing the final 2Fo-Fc electron density around the AMPPNP-Mn^{2+} complex contoured at the 1 σ level (gray mesh) and the anomalous difference Fourier map contoured at the 5 σ level (green mesh), indicating the position of the Mn^{2+} ion. AMPPNP is shown as sticks and colored by atom type as before. The Mn^{2+} ion (purple) and two coordinating water molecules (cyan) are shown as spheres. The orientation is the same as in Figure 3A left panel.

D. CASK^{WT} CaM-kinase domain in complex with co-purified 3′-AMP (21). Color-coding as above. The orientations are the same as in Figure 3B left panel.

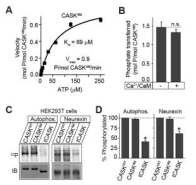

Figure 5. Compensation for slow kinetics in CASK kinase activity

A. Catalytic kinetics of CASK^{4M}. Purified CASK^{4M} CaM-kinase domain (2 μM) was incubated with increasing amount of γ^{32}P-ATP (400 cpm/pmol) in Tris-HCl buffer pH 7.0, containing Mg^{2+} (10 mM) and autocamtide (100 μM) as the substrate peptide for 10 min at 30°C. Amount of phospho-Autocamtide-2 generated was estimated by scintillation counting dot-blots on nitrocellulose membrane. Data shown are means ± SEMs (n=3). Michaelis constant (K ATP m) and V_{max} were calculated using Graph-Pad Prism software. Data shown are means ± SEMs (n=3).

B. Effect of Ca^{2+}/CaM on the catalytic rate. CASK^{4M} CaM-kinase domain (2μM) was incubated with γ^{32}P-ATP (200 μM, 800 cpm/pmol) in Tris-HCl buffer (pH 7.0) supplemented with Mg^{2+} (2 mM) and autocamtide-2 (100 μM), for 2 min in the presence or absence of Ca^{2+} (1 mM) and CaM (10 μM). Amount of phospho-autocamtide-2 generated was estimated with scintillation counting of dot blots on a nitrocellulose membrane. Data are represented as means ± SEMs, n = 3. n.s. (not significant)

C, D. Neurexin phosphorylation. HEK293T cells were transfected with Flag epitope-tagged neurexin and either EGFP-CASK, EGFP-CASK^{4M} or truncated EGFP-tCASK. 48 h later, transfected cells were labeled with $^{32}P_i$, followed by anti-Flag immunoprecipitation of neurexin. Immunoprecipitates were separated by SDS-PAGE and visualized by phosphorimager scanning. Autophosphorylation of the co-precipitated CASK (Autophos.) and phosphorylated neurexin (Neurexin) are shown. Immunoblotting (IB) for neurexin and CASK was performed to show expression. Bar-graph depicts the comparison of autophosphorylation or neurexin phosphorylation levels in cells co-expressing the indicated CASK variants. Data are represented as means ± SEMs, n = 3; asterisks indicate $P < 0.05$.

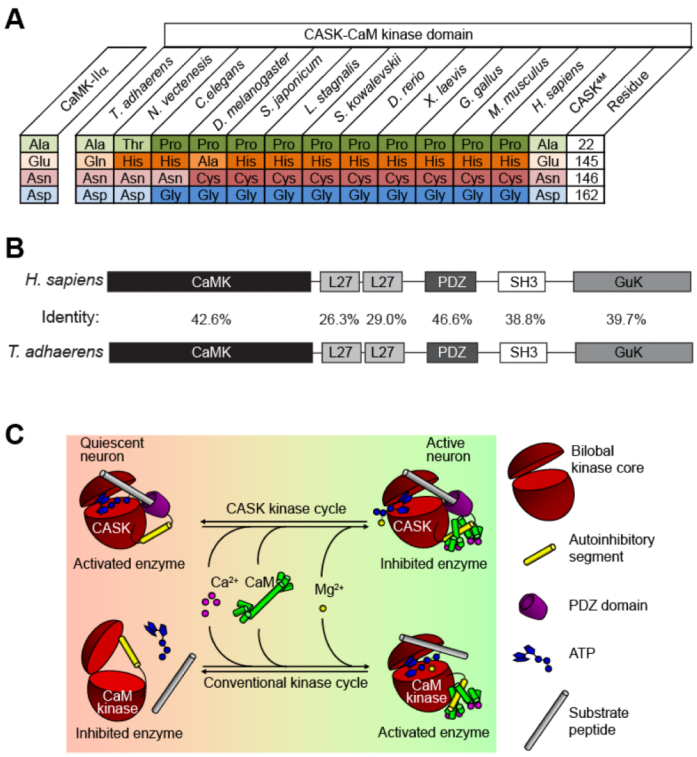

Figure 6. Evolution of CASK

A. Evolutionary changes in the nucleotide-binding pocket of CASK CaM-kinase domain. CASK CaM-kinase domain sequences from various animal species were aligned, and the residues corresponding to those mutated in CASK^{4M} were identified and are shown. Corresponding human CaMKIIα residues are shown on the left for comparison.

B. Sequence conservation (identities) of CASK domains between human and placozoan CASK (from *T. adhaerens*). See Supplemental Figure S7 for a full sequence alignment.

C. Model comparing CASK and CaMKII catalytic cycles. Typically, CaM-kinases are held in an autoinhibited conformation by the autoregulatory domain (yellow) with an open, inactive nucleotide binding cleft. Upon binding of Ca^{2+} (purple)/CaM (green), this autoinhibition is released and the enzyme attains an active closed conformation amenable to Mg^{2+} (yellow)/ATP (blue) binding and substrate binding (lower panel). CASK CaM-kinase, on other hand, constitutively binds ATP, and is regulated by the recruitment of its substrates via the MAGUK scaffolding domains, especially the PDZ-domain.

Table 1

Crystallographic Data and Refinement

Data Collection	**Native**	**AMPPNP**	**Mn^{2+}**	**AMPPNP-Mn^{2+}**
Wavelength (Å)	0.91841	0.91841	1.87856	1.87856
Temperature (K)	100	100	100	100
Space Group	$P2_12_12_1$	$P2_12_12_1$	$P2_12_12_1$	$P2_12_12_1$
Unit Cell (Å) *a, b, c*	58.7, 61.8, 100.2	59.0, 62.2, 97.9	58.9, 61.8, 101.5	58.9, 62.0, 100.6
Resolution (Å)	30.0-1.95	50.0-2.05	50.0-2.20	20.0-2.30
	(1.98-1.95)[a]	(2.09-2.05)	(2.24-2.20)	(2.36-2.30)
Reflections				
Unique	26982 (1269)	22576 (1094)	35224 (1513)[b]	31058 (1968)[b]
Completeness (%)	98.4 (94.7)	97.7 (97.4)	96.9 (84.4)	98.2 (83.8)
Redundancy	6.7 (6.1)	5.2 (4.9)	4.7 (2.7)	4.5 (2.7)
I/σ(I)	29.0 (1.9)	15.9 (2.3)	11.3 (1.3)	14.4 (2.2)
R_{sym}(I) *c*	3.6 (68.4)	5.7 (66.4)	9.0 (56.8)	6.3 (49.7)
Refinement				
Resolution (Å)	30.0-2.00	30.0-2.10	30.0-2.20	20.0-2.30
	(2.05-2.00)	(2.15-2.10)	(2.26-2.20)	(2.36-2.30)
Reflections				
Number	24959 (1727)	21153 (1516)	18858 (1180)	16714 (1046)
Completeness (%)	98.6 (94.3)	97.7 (96.6)	97.0 (84.2)	100.0 (100.0)
Test Set (%)	5.1	5.1	5.1	5.0
R_{work} *d*	19.6 (24.8)	21.9 (29.7)	21.0 (28.5)	17.9 (20.9)
R_{free} *d*	24.1 (31.5)	26.8 (29.6)	27.0 (39.9)	23.4 (30.9)
ESU (Å)[e]	0.14	0.20	0.19	0.17
Refined Atoms				
Protein	2461	2446	2422	2430
Water	235	199	141	196
Ligands	19	31	-	32
Mean B-Factors (Å^2)				
Wilson	30.4	33.7	35.1	51.1
Protein	38.0	46.1	35.6	43.1
Water	46.2	46.3	38.5	46.9
Ligand	65.5	63.5	-	54.2
Ramachandran Plot (%) *f*				
Favored	96.0	94.4	97.0	95.7
Outliers	1.0	1.0	0.7	1.0
RMSD[a] Target Geometry				
Bond Lengths (Å)	0.011	0.011	0.010	0.010

Data Collection	**Native**	**AMPPNP**	**Mn^{2+}**	**AMPPNP-Mn^{2+}**
Bond Angles (°)	1.322	1.209	1.248	1.324
RMSD B-Factors ($Å^2$)				
Main Chain Bonds	0.661	0.437	0.549	0.589
Main Chain Angles	1.064	0.741	0.942	1.033
Side Chain Bonds	1.554	1.099	1.316	1.523
Side Chain Angles	2.277	1.719	2.110	2.493
PDB ID	XXXX	XXXX	XXXX	XXXX

[a] Data for the highest resolution shell in parentheses

[b] Mn^{2+} and AMPPNP-Mn^{2+} data sets were processed without merging Friedel pairs

[c] $R_{sym}(I) = \sum_{hkl}\sum_i|I_i(hkl) - \langle I(hkl)\rangle| / \sum_{hkl}\sum_i|I_i(hkl)|$; for n independent reflections and i observations of a given reflection; $\langle I(hkl)\rangle$ - average intensity of the i observations

[d] $R = \sum_{hkl}||F_{obs}| - |F_{calc}|| / \sum_{hkl}|F_{obs}|$; R_{work} - $hkl \notin T$; R_{free} - $hkl \in T$; T test set

[e] ESU - estimated overall coordinate error based on maximum likelihood

[f] Calculated with MolProbity (http://molprobity.biochem.duke.edu/)

[g] RMSD - root-mean-square deviation